MECSOL 2019 - Proceedings of the 7th International Symposium on Solid Mechanics
V. Tita, A. Ferreira, M.L. Ribeiro, A. Vieira and A.T. Beck (Editors), ABCM, Sao Carlos, SP, Brazil, April 15th to 17th, 2019

Strain-based fatigue life predictions using measured and estimated material parameters

Caio Ferreira Barros[1], Jorge Alberto Rodriguez Duran[1]

[1] Universidade Federal Fluminense – Escola de Engenharia Industrial Metalúrgica de Volta Redonda (EEIMVR-UFF), Programa de Pós-graduação em Engenharia Mecânica (PGMEC), Av. dos Trabalhadores, 420, Vila Santa Cecília – Volta Redonda / RJ, 27255-125

Abstract. The fatigue life can be calculated from local strain amplitudes according to the well known Coffin-Manson relation. For notched bodies, neglecting hardening and softening transients, local strains should follow simultaneously the cyclic stress-strain curve and a stress concentration rule. Occasionally, the fitting constants for the cyclic stress-strain curve are not available and the so called compatible constants are used instead. The compatible constants are calculated from the cyclic constants fitted to the strain-life curve. The present paper evaluates the consequences that this decision have on the final life calculated with the strain-based approach to fatigue and how divergent are the results generated according to the material and analysis parameters. The fatigue life results obtained with the compatible constants for aluminum show considerable divergence in relation to the results obtained with the experimental constants, which varies according to the values of the other parameters of the analysis, such as stress amplitude S_a, stress ratio R and stress concentration factor k_t. Between the results, stand out the highly conservative results for lives less than 10^5 cycles in combinations of $R \geq 0$ and $k_t \geq 3$, as well as the non-conservative results for analysis performed with $R \geq 0$, especially for lives greater than 10^5 cycles. Therefore, in these contexts it is not recommended to use compatible constants.
Keywords: strain-based approach to fatigue, aluminum fatigue, cyclic stress-strain constants, strain-life constants, compatible constants

INTRODUCTION

Through the strain-based approach to fatigue, life can be calculated from strain amplitude through the strain-life curve. Determined from the material properties, the strain-life curve, which relates local strain amplitude and life, represented in number of cycles to failure, is described by the Coffin-Manson relation, Eq. (1). Where ε_a is the strain amplitude, N_f is the number of cycles to failure, and the remaining constants are the material properties: modulus of elasticity E, fatigue strength coefficient σ'_f, fatigue strength exponent b, fatigue ductility coefficient ε'_f and fatigue ductility exponent c.

$$\varepsilon_a = \frac{\sigma'_f}{E}(2N_f)^b + \varepsilon'_f(2N_f)^c \tag{1}$$

For the cases with notched components, which are analyzed in this paper, a stress concentration rule must be used in order to add the effects caused by the notch on the life and to verify how the change in the stress concentration factor modifies the obtained results. The stress concentration rule used was Neuber's rule, described by Eq. (2). Where σ_a and ε_a are the local stress and strain amplitudes, respectively, S_a is the nominal stress amplitude, k_t is the stress concentration factor and E is modulus of elasticity.

$$\sigma_a \varepsilon_a = \frac{(k_t S_a)^2}{E} \tag{2}$$

In order to include the stress concentration rule in the life analysis, the strain amplitude must be adjusted to include it. Therefore, the stress concentration rule is used in relation to the cyclic stress-strain curve, which is described by the Ramberg-Osgood relation, Eq. (3). Where, again, σ_a and ε_a are the local stress and strain amplitudes, respectively, E is modulus of elasticity, and the remaining values are the cyclic constants: cyclic strength coefficient H' and cyclic strain hardening exponent n'. Thus, resulting in a strain amplitude value that represents a certain combination of load and notch geometry, which is then used to calculate the life.

$$\varepsilon_a = \frac{\sigma_a}{E} + \left(\frac{\sigma_a}{H'}\right)^{1/n'} \tag{3}$$

Between the relations proposed by Coffin-Manson, Eq. (1), and by Ramberg-Osgood, Eq. (3), there are six constants that are material properties directly extracted from fatigue experiments. However, literature shows in Dowling (2012),

Hertzberg et al. (1996) and Stephens et al. (2001) that, through relations between the cyclic curves' constitutive equations, there is a mathematical relation that provides two of these constants from the others. Nominally, H' and n' from σ'_f, b, ε'_f and c. These relations are defined by Eq. (4) and (5).

$$H' = \frac{\sigma'_f}{\left(\varepsilon'_f\right)^{b/c}} \tag{4}$$

$$n' = \frac{b}{c} \tag{5}$$

Since all six constants are essential for the calculation of fatigue life, the possibility to obtain two constants from the remaining through a mathematical approach is considerably interesting. Specially considering that material's cyclic properties are not always readily available and that the financial and time cost to perform the experiments and analyze the results are high.

For some cases, the use of the mathematical approach to obtain the, so called, compatible constants can result in fatigue life values equivalent to those that would be obtained with only experimental constants. However, the compatibility condition is not always ensured, as shown in Niesłony et al. (2008, 2012) and supported by the results presented in Kim et al. (2002).

The fatigue life results obtained for steels with both experimental and compatible constants are usually quite equivalent, as shown in the study performed by Meggiolaro & Castro (2004). However, for aluminum, there is a deviation that must be considered.

Similarly to the studies presented previously that analyze the same method as the present paper, recent studies have been interested on the reliability of results obtained with estimated cyclic constants for both the cyclic stress-strain curve and strain-life curve. As in Basan et al. (2011, 2015); Marohnić et al. (2015), where the authors verify that the same method does not generates consistent results for every material type and life range. Kim et al. (2002); Troshchenko & Khamaza (2010) did similar verifications about multiple methods, but they also directly compared the fatigue life results obtained with experimental and estimated constants.

Likewise, new approachs have been studied to estimate the cyclic properties from readily available material properties. Such as the method proposed in Basan et al. (2010a,b) to estimate cyclic stress-strain constants from Brinnell hardness HB. Meggiolaro & Castro (2004) proposed a method to estimate the strain-life constants from median value of the properties for each material group. Niesłony et al. (2008) proposed a 3D method, using a stress-strain-life graph, that simultaneously ensure the compatibility condition between the cyclic stress-strain curve and the strain-life curve. The studies performed in Tomasella et al. (2011); Troshchenko et al. (2011) proposed the use of neural networks to estimate cyclic constants.

Therefore, the objective of this paper is to investigate how the fatigue life results for aluminum, obtained through the strain-based approach for notched bodies, change with the use of compatible constants by comparing them to the results obtained with experimental constants. As well as identify the combinations of parameters that cause non-equivalent results, specially the non-conservative.

ANALYSIS PROCEDURE

Regarding the analysis parameters, there are two main areas covered by the analysis: load and geometry. For loads, the control parameters were stress intensity and stress ratio. For geometry, the control parameter was stress concentration factor. In order to extract the maximum amount of results, multiple combinations between the values of each parameter were used.

The combinations of nominal stress amplitude S_a and nominal maximum stress S_{max} used in the analysis represent loads with stress ratio R within the limits of -1 and 0.5, which represent a wide and typical range of ratios. Between those limits, four values were used for R: -1, -0.5, 0 and 0.5. Regarding the stress intensity, ten pairs of S_a and S_{max} were used for each R, following the relation established in Eq. (6). These pairs were limited simultaneously at both values, S_a was limited to 30% of ultimate tensile strength σ_u and S_{max} was limited to 70% of this same value.

$$S_{max} = \frac{2S_a}{1-R} \tag{6}$$

In order to demonstrate the influence of the notch on the calculated fatigue lives, typical values were selected for the stress concentration factor k_t. These values were: 2, 3 and 4.

Regarding the materials, 50 variations of aluminum were used for the analysis. All the materials and their properties are referenced at Tab. 1. These properties were sourced from Boller & Seeger (1987); Burk & Lawrence (1978); Chen & Lawrence (1979); Dowling (2012); Lease & Stephens (1991); SAE Standard J1099 (1998); Wong (1984).

Table 1: Material properties of all aluminum used for the analysis.

Material	σ_0 (MPa)	σ_u (MPa)	E (MPa)	H' (MPa)	n'	σ'_f (MPa)	b	ε'_f	c
1100	–	110	69000	154	0.144	166	– 0.096	1.643	– 0.669
1100 Al	97	110	69050	184	0.159	159	– 0.092	0.467	– 0.613
2014-T6	–	483	72700	605	0.049	976	– 0.12	0.88	– 0.88
2014-T6	–	510	69000	963	0.132	1008	– 0.114	1.418	– 0.87
2014-T6	463	511	69050	704	0.072	776	– 0.091	0.269	– 0.742
2024-T3	345	490	70280	843	0.109	835	– 0.096	0.174	– 0.644
2024-T3	378	486	74500	590	0.04	1044	– 0.114	1.765	– 0.927
2024-T3	378	486	74500	590	0.04	3148	– 0.247	0.069	– 0.634
2024-T3	378	486	82000	590	0.04	1044	– 0.114	1.765	– 0.927
2024-T351	379	469	73100	662	0.07	927	– 0.113	0.409	– 0.713
2024-T4	304	476	70430	808	0.098	764	– 0.075	0.334	– 0.649
2024-T4	303	476	73100	738	0.08	1294	– 0.142	0.327	– 0.645
5083-0	–	294	71000	580	0.114	711	– 0.122	0.405	– 0.692
5083-H12	–	385	69000	417	0.035	650	– 0.094	2.26	– 1.01
5183-0	–	299	71000	507	0.072	638	– 0.107	0.581	– 0.89
5454	–	334	69000	373	0.047	554	– 0.089	0.31	– 0.62
5456-H311	–	400	69000	817	0.145	826	– 0.115	1.076	– 0.797
5456-H311	235	400	69050	636	0.084	702	– 0.102	0.2	– 0.655
6061-T6	–	314	69600	426	0.062	535	– 0.082	1.34	– 0.83
6061-T6	–	340	72700	416	0.042	645	– 0.097	0.22	– 0.6
6061-T6	–	389	69000	422	0.03	689	– 0.094	0.35	– 0.67
7075-T6	–	572	72230	521	0.045	776	– 0.0951	2.56	– 0.987
7075-T6	–	579	71000	2514	0.146	1917	– 0.176	0.156	– 0.526
7075-T6	469	578	71000	977	0.106	1466	– 0.143	0.262	– 0.619
7075-T6	470	580	71120	913	0.088	886	– 0.076	0.446	– 0.759
7075-T6	512	572	70940	1499	0.186	1048	– 0.106	3.1357	– 1.045
7075-T6	512	572	72230	521	0.045	776	– 0.095	2.565	– 0.987
7075-T651	–	580	70000	852	0.074	1231	– 0.122	0.263	– 0.806
7075-T7351	382	462	71000	695	0.094	989	– 0.14	6.812	– 1.198
7175-T73	–	524	71300	529	0.033	765	– 0.082	6.18	– 1.14
7475-T761	414	475	70010	675	0.059	983	– 0.107	4.246	– 1.066
A356-T6	–	252	71000	394	0.0615	495	– 0.117	0.0177	– 0.458
A356-T6	–	266	70000	383	0.0499	502	– 0.119	0.0166	– 0.544
A356-T6	–	283	70000	379	0.0429	594	– 0.124	0.0269	– 0.53
Al 99.5	19	73	70000	255	0.265	95	– 0.088	0.022	– 0.328
Al 99.5	19	73	70000	453	0.337	117	– 0.109	0.017	– 0.315
AlCuMg2	275	446	74100	648	0.062	687	– 0.074	0.514	– 0.83
AlCuMg2	396	490	73300	557	0.039	782	– 0.082	0.197	– 0.644
AlCuMg2	476	490	73300	669	0.074	891	– 0.103	4.206	– 1.056
AlCuMg2	88	245	74600	453	0.201	314	– 0.091	0.162	– 0.452
AlMg4.5Mn	226	348	85000	450	0.056	906	– 0.148	52.058	– 1.441
AlMg4.5Mn	298	363	71500	1103	0.22	1576	– 0.201	1.303	– 0.879
AlMg4.5Mn	298	363	71500	535	0.07	629	– 0.086	0.329	– 0.684
AlMg4.5Mn	298	363	71500	561	0.08	723	– 0.108	1.613	– 0.871
AlMg4.5Mn	298	363	71500	693	0.125	654	– 0.089	0.45	– 0.755

Table 1: Material properties of all aluminum used for the analysis. (Continued.)

Material	σ_0 (MPa)	σ_u (MPa)	E (MPa)	H' (MPa)	n'	σ'_f (MPa)	b	ε'_f	c
AlMg4.5Mn	298	363	71500	777	0.137	546	– 0.07	0.034	– 0.436
AlMgSi0.8	157	260	66700	392	0.06	481	– 0.084	1.095	– 0.867
AlMgSi0.8	294	329	67200	451	0.05	542	– 0.075	0.7	– 0.816
AlMgSi1	250	348	74500	454	0.052	445	– 0.054	0.116	– 0.641
AlMgSi1	348	383	74550	478	0.046	554	– 0.068	5.375	– 1.208

Therefore, the analysis was performed individually on each material for each value of k_t and combinations of S_a and S_{max}, following the general procedure to calculate lives detailed in the introduction. With exception of the cases with mean stress σ_m different than zero, because, for these cases, σ_m must be included in the calculation of fatigue life. For such cases, the Coffin-Manson equation, Eq. (1), was substituted by the modified Morrow approach, Eq. (7), which includes the mean stress σ_m at the elastic portion of the equation.

$$\varepsilon_a = \frac{\sigma'_f}{E}\left(1 - \frac{\sigma_m}{\sigma'_f}\right)(2N_f)^b + \varepsilon'_f\,(2N_f)^c \tag{7}$$

RESULTS

The Fig. 1 presents a comparison between the life results obtained with the calculated constants $N_{f\,calc}$ and the experimental constants $N_{f\,exp}$ in order to verify if there is any divergence in the results obtained with all possible combination of analysis parameters.

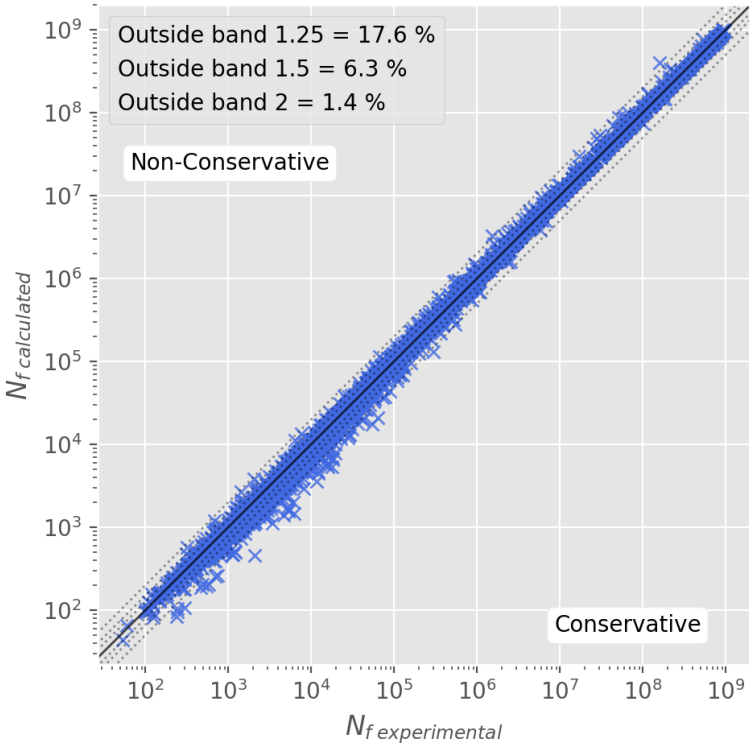

Figure 1 – General fatigue life results for aluminum.

For such graph, the life results obtained with the compatible and experimental constants were used as coordinates in a log-log graph. Accompanied by a reference line that represent where the lives are equivalent and scatter bands of factor 1.25, 1.5 and 2, as well as, the proportion of results outside each scatter band.

It is promptly observed that there is divergence between the results, especially in the low life region, where the results obtained with the calculated constants are more conservative. Among the available data, 17.6% of all results are outside the 1.25 scatter band, and focusing only in the low life region, an even greater proportion of the results are outside the considered scatter bands.

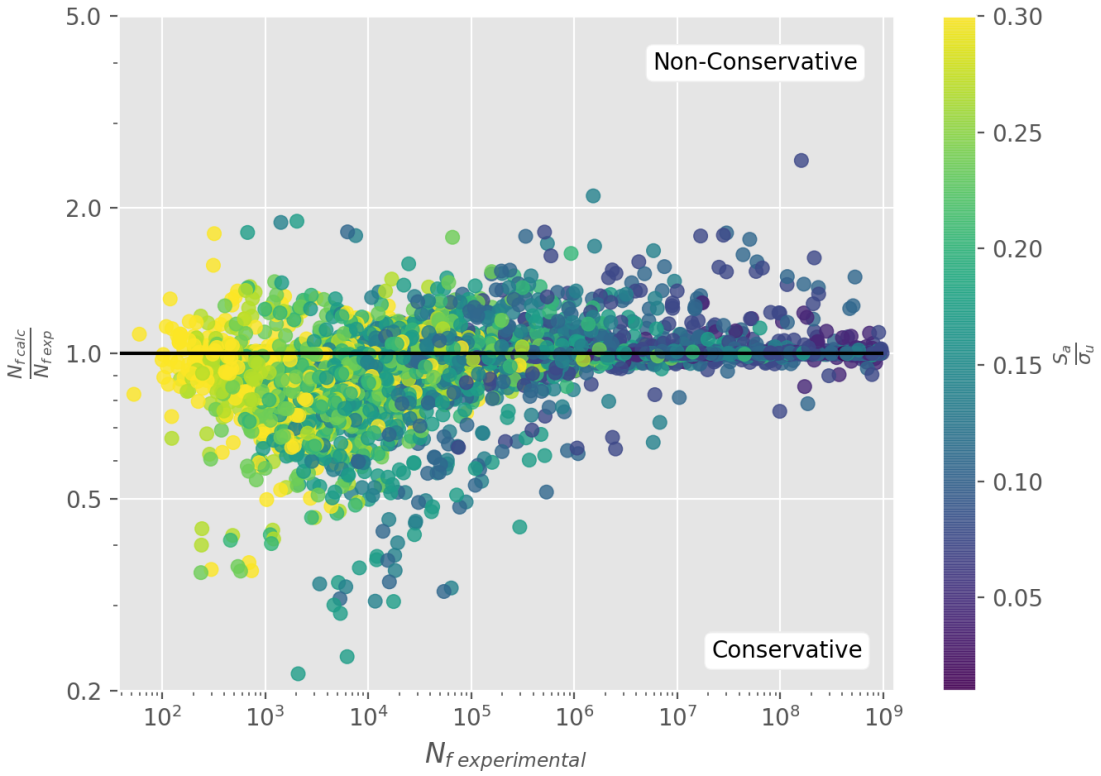

Figure 2 – Relation between $N_{f\,calc}/N_{f\,exp}$, $N_{f\,exp}$ and S_a/σ_u for all analysis parameters.

The Fig. 2 presents the relation between the ratio between the results, represented by $N_{f\,calc}/N_{f\,exp}$, and the lives calculated with the experimental constants $N_{f\,exp}$, supported by a color bar that represents the stress amplitude S_a normalized between all material by σ_u. This graph shows how the ratio between the calculated lives behave throughout the life range considered in the analysis and the color bar shows the direct relation that exists between the increase in stress amplitude and the decrease in fatigue life. It is observed at Fig. 2 that the largest deviations, which are in the order of two to five times, occur for short lives and that they are mostly conservative. Also, for lives greater than 2 x 10^6 cycles most results are either equivalent or non-conservative.

In order to observe the results more carefully, Fig. 3 and 4 show the same relation $N_{f\,exp}$ vs. $N_{f\,calc}/N_{f\,exp}$ as Fig. 2, only this time, the results are separated by stress ratio R and stress concentration factor k_t. A trend line was added to these graphs in order to increase their readability. For which, the mean values $\overline{X}_{geom}$ were calculated for each section of the data set with Eq. (8), where n is the sample size and x_i is the current value. Such equation was used because, as the data is being evaluated about an equivalence line in a log axis, it's necessary that equivalent points, above and below it, have the same weight.

$$\overline{X}_{geom} = \left(\prod_{i=1}^{n} x_i\right)^{1/n} = \exp\left(\frac{1}{n}\sum_{i=1}^{n}\ln(x_i)\right) \tag{8}$$

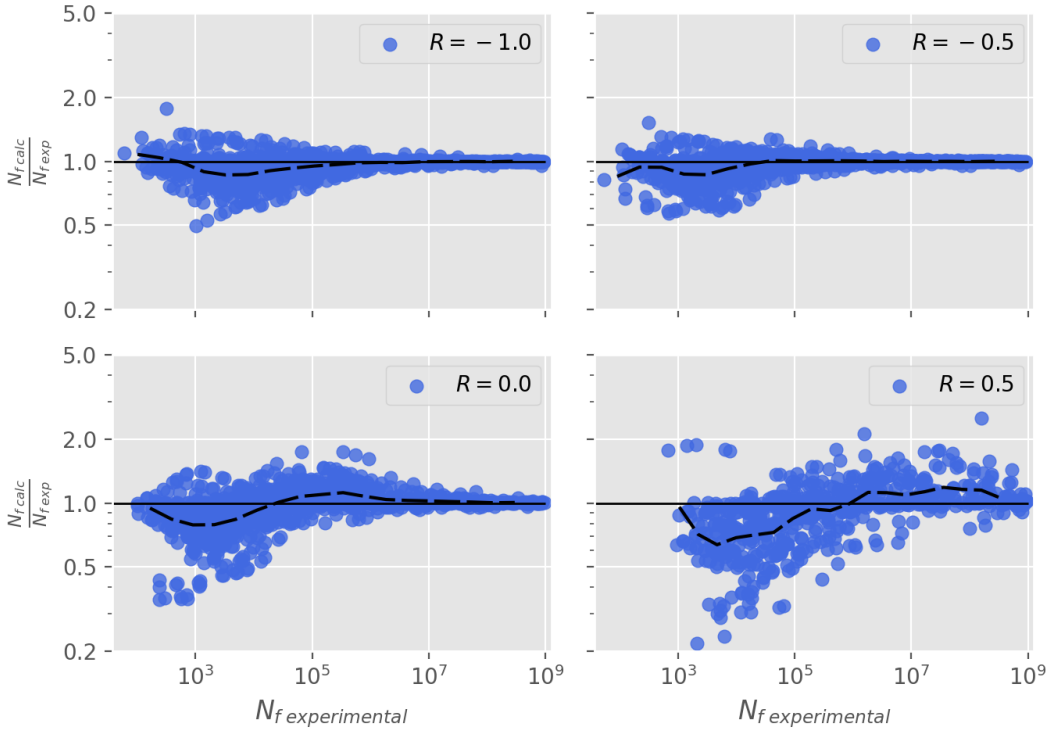

Figure 3 – Relation between $N_{f\,calc}/N_{f\,exp}$ and $N_{f\,exp}$ separated by R.

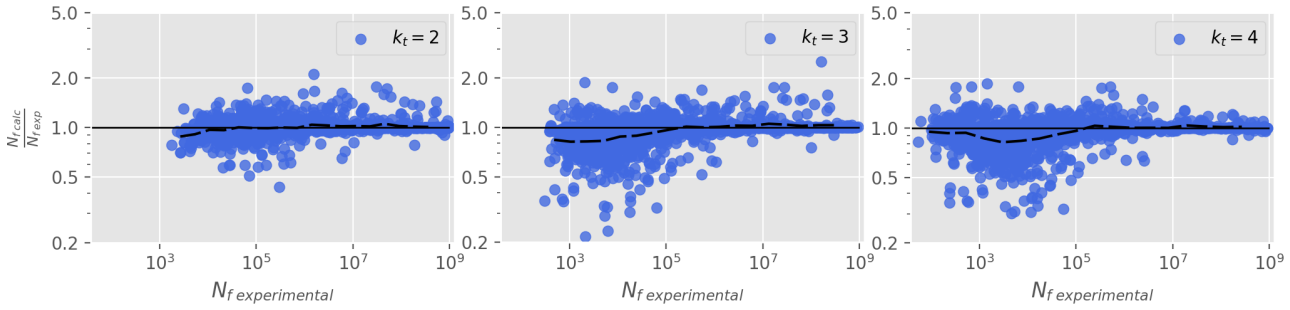

Figure 4 – Relation between $N_{f\,calc}/N_{f\,exp}$ and $N_{f\,exp}$ separated by k_t.

The Fig. 3 shows the increase of the divergence between the obtained results accompanying the increase of R. The results for short lives are increasingly conservative and the results for long lives are increasingly non-conservative. The results for $R = -1.0$ and -0.5 are very similar. For both these stress ratios, the results are slightly conservative for short lives and after, approximately, 10^5 cycles the results are equivalent. For $R = 0.0$ and 0.5, the results are even more conservative for short lives, but non-conservative for lives greater than 10^5.

The increase of k_t, shown in Fig. 4, does not equate to an increase in the deviation between methods. Similar results occur at similar lives for different k_t.

Detailed numerical analysis of the results are presented in Tab. 2, 3, 4 and 5 separated by stress ratio R. These results are plotted at Fig. 5 and 6. Through these tables and figures, it is possible to observe more objectively the effects caused by the change in each of the analysis parameters.

For each group of results, the analysis presented in the tables contain the sample size n, the geometric mean $\overline{X}_{geom}$ and

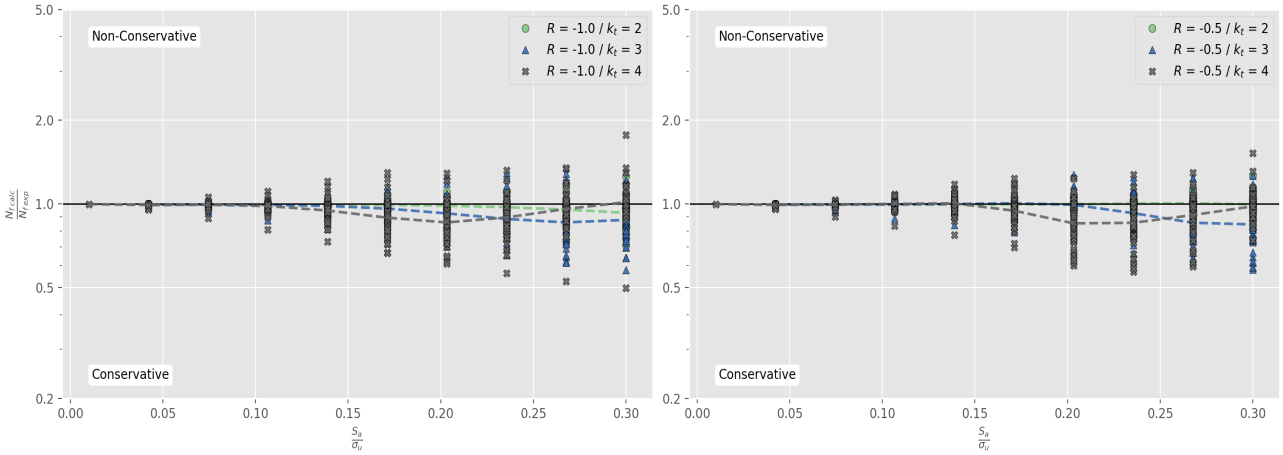

Figure 5 – Relation between $N_{f\,calc}/N_{f\,exp}$ and stress amplitude for R = – 1 and – 0.5 and k_t = 2, 3 and 4.

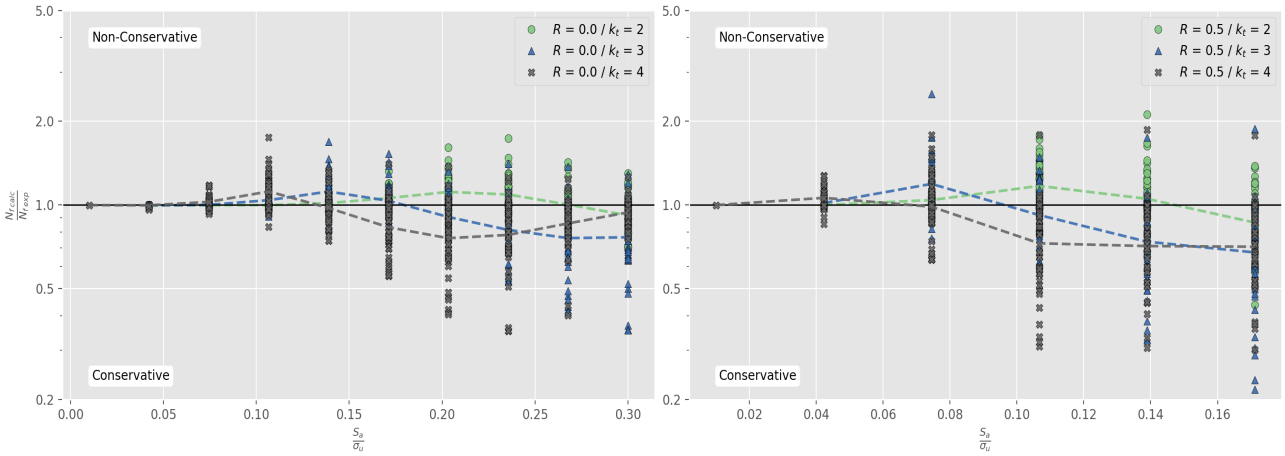

Figure 6 – Relation between $N_{f\,calc}/N_{f\,exp}$ and stress amplitude for R = 0.0 and 0.5 and k_t = 2, 3 and 4.

Table 2 – Statistical analysis for R = – 1.

S_a/σ_u	$R=-1, k_t=2$			$R=-1, k_t=3$			$R=-1, k_t=4$		
	n	$\overline{X}_{geom}$	S_{geom}	n	$\overline{X}_{geom}$	S_{geom}	n	$\overline{X}_{geom}$	S_{geom}
0.01	0	–	–	0	–	–	1	0.999	1
0.04	3	0.995	1.006	6	0.995	1.010	13	0.991	1.016
0.07	9	0.995	1.011	33	0.995	1.016	42	0.994	1.025
0.11	30	0.995	1.016	45	0.993	1.028	50	0.983	1.047
0.14	41	0.994	1.022	50	0.984	1.045	50	0.947	1.092
0.17	49	0.992	1.030	50	0.962	1.074	50	0.893	1.146
0.20	50	0.986	1.043	50	0.925	1.116	50	0.858	1.184
0.24	50	0.974	1.060	50	0.884	1.155	50	0.895	1.172
0.27	50	0.955	1.083	50	0.859	1.183	50	0.960	1.153
0.30	50	0.929	1.112	50	0.876	1.180	50	1.016	1.168

Table 3 – Statistical analysis for R = – 0.5.

S_a/σ_u	$R=-0.5,\ k_t=2$			$R=-0.5,\ k_t=3$			$R=-0.5,\ k_t=4$		
	n	$\overline{X}_{geom}$	S_{geom}	n	$\overline{X}_{geom}$	S_{geom}	n	$\overline{X}_{geom}$	S_{geom}
0.01	0	–	–	0	–	–	1	0.999	1
0.04	3	0.995	1.006	6	0.995	1.009	14	0.992	1.015
0.07	9	0.995	1.010	34	0.996	1.014	45	0.996	1.019
0.11	33	0.996	1.013	49	0.996	1.021	50	1.000	1.039
0.14	41	0.995	1.018	50	1.000	1.037	50	1.005	1.077
0.17	49	0.996	1.024	50	1.006	1.056	50	0.946	1.127
0.20	50	0.999	1.035	50	0.994	1.106	50	0.852	1.183
0.24	50	1.004	1.047	50	0.927	1.134	50	0.856	1.195
0.27	50	1.006	1.066	50	0.856	1.179	50	0.913	1.163
0.30	50	0.997	1.101	50	0.844	1.199	49	0.981	1.120

Table 4 – Statistical analysis for R = 0.

S_a/σ_u	$R=0,\ k_t=2$			$R=0,\ k_t=3$			$R=0,\ k_t=4$		
	n	$\overline{X}_{geom}$	S_{geom}	n	$\overline{X}_{geom}$	S_{geom}	n	$\overline{X}_{geom}$	S_{geom}
0.01	0	–	–	0	–	–	1	0.999	1
0.04	3	0.996	1.005	7	0.997	1.007	20	0.997	1.011
0.07	12	0.998	1.007	38	1.001	1.015	49	1.026	1.047
0.11	36	0.999	1.013	50	1.041	1.062	50	1.119	1.151
0.14	49	1.016	1.033	50	1.118	1.145	50	0.975	1.149
0.17	50	1.059	1.076	50	1.036	1.147	50	0.832	1.225
0.20	50	1.114	1.137	50	0.906	1.173	48	0.760	1.323
0.24	50	1.091	1.155	50	0.814	1.243	48	0.781	1.327
0.27	50	1.004	1.146	49	0.760	1.315	47	0.858	1.229
0.30	50	0.917	1.167	48	0.765	1.337	45	0.940	1.102

Table 5 – Statistical analysis for R = 0.5.

S_a/σ_u	$R=0.5,\ k_t=2$			$R=0.5,\ k_t=3$			$R=0.5,\ k_t=4$		
	n	$\overline{X}_{geom}$	S_{geom}	n	$\overline{X}_{geom}$	S_{geom}	n	$\overline{X}_{geom}$	S_{geom}
0.01	0	–	–	0	–	–	1	0.999	1
0.04	3	1.000	1.005	10	1.016	1.018	35	1.061	1.090
0.07	24	1.042	1.067	50	1.191	1.250	50	0.986	1.268
0.11	49	1.171	1.206	50	0.920	1.287	48	0.728	1.434
0.14	50	1.052	1.262	48	0.738	1.422	45	0.712	1.405
0.17	50	0.864	1.317	48	0.675	1.521	41	0.708	1.407

the geometric deviation S_{geom}. The mean was calculated with Eq. (8) and the deviation with Eq. (9).

$$S_{geom} = \exp\left(\sqrt{\frac{1}{n-1}\sum_{i=1}^{n}\left(\ln\left(\frac{x_i}{\overline{X}_{geom}}\right)\right)^2}\right) \tag{9}$$

Each figure shows on its vertical axis the ratio N_{fcalc}/N_{fexp}, represented in logarithmic scale, and on its horizontal axis the normalized stress amplitude S_a/σ_u. Similarly to previous figures, trend lines are also plotted, which represent the calculated means presented in Tab. 2, 3, 4 and 5.

From the increase of R, can be observed the increase in the divergence between the results considering the same value for other parameters, as already shown before. However, the results are separated by all parameters for this observation.

So, regardless of the other parameters, for $R = -1.0$ and -0.5 all results are either slightly conservative or equivalent, noting that for $k_t = 2$ all results are equivalent. Non-conservative results are shown for $R = 0.0$ and 0.5 for all k_t, but for different stress amplitude.

Regarding k_t, can be observed that its increase causes the curves to dislocate to lower values of stress amplitude without major alterations to the deviation. At Fig. 4, it is observed that similar deviations occur at the same life for different k_t values. This means that k_t does not impact the deviations, but it reduces the intensity of stress needed for similar deviations at a certain life.

The increase of S_a/σ_u is generally accompanied by the increase of the divergence between results. Which is equivalent to the relation observed previously that greater deviations are observed at shorter lives. Non-conservative results are spread throughout the stress amplitude range because they depend on other parameters, such as the stress concentration factor.

CONCLUSIONS

From the study carried out in this paper, using well established equations for the solutions, fatigue life was calculated for aluminum through the strain-based approach to fatigue with compatible and experimental constants. Then, these results were presented accompanied by a discussion about how they behave according to the parameters of the analysis.

Through a direct comparison between the life results obtained with the compatible and experimental cyclic stress-strain constants, it was observed that there is deviation between them and that they should be examined more carefully. After that, the results were broken down by the parameters, in order to enable an in depth analysis of the impact of each one of them.

Different observations can be made about each parameter. About stress ratio R, it can be concluded that it is the main parameter responsible for the change in the divergence of the results. The variation of stress concentration factor k_t did not cause changes in the divergence, but it enabled similar divergence to occur for lower stresses, while maintaining the same life. About life, which is directly related to stress amplitude S_a, there are two main regions in the results: one below 2 x 10^6 that includes mainly conservative results and another, above this threshold, that includes mainly equivalent results.

Through the analysis of the results, there are some outstanding situations due to their undesirable results. Firstly, non-conservative results are found at long lives for analyses performed with $R \geq 0$, specially for lives greater than 10^5. Also, for lives less than 10^5 associated with $R \geq 0$ and $k_t \geq 3$, there are greatly conservative results.

Therefore, even though it's hard to establish a general rule about the use of compatible constants for aluminum, because of the particular result generated by each combination of analysis' parameters, there are some combinations of parameters that generate unwanted results (non-conservative or extremely conservative) that should be avoided.

REFERENCES

Basan, R., Franulović, M., Prebil, I., & Črnjarić Žic, N. (2011). Analysis of strain-life fatigue parameters and behaviour of different groups of metallic materials. *International Journal of Fatigue*, 33(3), 484 – 491.

Basan, R., Franulović, M., & Smokvina Hanza, S. (2010a). Estimation of cyclic stress-strain curves for low-alloy steel from hardness. 49.

Basan, R., Rubeša, D., Franulović, M., & Križan, B. (2010b). A novel approach to the estimation of strain life fatigue parameters. *Procedia Engineering*, 2(1), 417 – 426. Fatigue 2010.

Basan, R., Rubeša, D., Franulović, M., & Marohnić, T. (2015). Some considerations on the evaluation of methods for the estimation of fatigue parameters from monotonic properties. *Procedia Engineering*, 101, 18 – 25. 3rd International Conference on Material and Component Performance under Variable Amplitude Loading, VAL 2015.

Boller, C. & Seeger, T. (1987). *Materials data for cyclic loading*, volume 42. Amsterdam: Elsevier.

Burk, J. D. & Lawrence, F. V. (1978). *The Effect of Residual Stresses on Weld Fatigue Life*. Technical report, University of Illinois.

Chen, W.-C. & Lawrence, F. V. (1979). *A Model for Joining the Fatigue Crack Initiation and Propagation Analyses*. Technical report, University of Illinois.

Dowling, N. E. (2012). *Mechanical behavior of materials: engineering methods for deformation, fracture, and fatigue*. Boston, MA: Pearson, fourth edition.

Hertzberg, R. W., Vinci, R. P., & Hertzberg, J. L. (1996). *Deformation and fracture mechanics of engineering materials*. New York: John Wiley & Sons, fourth edition.

Kim, K., Chen, X., Han, C., & Lee, H. (2002). Estimation methods for fatigue properties of steels under axial and torsional loading. *International Journal of Fatigue*, 24(7), 783 – 793.

Lease, K. & Stephens, R. (1991). *Verification of variable amplitude fatigue life methodologies for a cast aluminum alloy*.

Technical report, SAE Technical Paper.

Marohnić, T., Basan, R., & Franulović, M. (2015). Evaluation of the possibility of estimating cyclic stress-strain parameters and curves from monotonic properties of steels. *Procedia Engineering*, 101(Supplement C), 277 – 284.

Meggiolaro, M. & Castro, J. (2004). Statistical evaluation of strain-life fatigue crack initiation predictions. *International Journal of Fatigue*, 26(5), 463 – 476.

Niesłony, A., el Dsoki, C., Kaufmann, H., & Krug, P. (2008). New method for evaluation of the manson–coffin–basquin and ramberg–osgood equations with respect to compatibility. *International Journal of Fatigue*, 30(10), 1967 – 1977.

Niesłony, A., Kurek, A., el Dsoki, C., & Kaufmann, H. (2012). A study of compatibility between two classical fatigue curve models based on some selected structural materials. *International Journal of Fatigue*, 39, 88 – 94. Physical and phenomenological approaches to fatigue damage.

SAE Standard J1099 (1998). *Technical Report on Low Cycle Fatigue Properties Ferrous and Non-Ferrous of Materials*. Technical report, SAE International.

Stephens, R. I., Fatemi, A., Stephens, R. R., & Fuchs, H. O. (2001). *Metal fatigue in engineering*. New York: John Wiley & Sons, second edition.

Tomasella, A., el Dsoki, C., Hanselka, H., & Kaufmann, H. (2011). A computational estimation of cyclic material properties using artificial neural networks. *Procedia Engineering*, 10, 439 – 445. 11th International Conference on the Mechanical Behavior of Materials (ICM11).

Troshchenko, V. & Khamaza, L. (2010). Strain–life curves of steels and methods for determining the curve parameters. part 1. conventional methods. *Strength of materials*, 42(6), 647–659.

Troshchenko, V. T., Khamaza, L. A., Apostolyuk, V. A., & Babich, Y. N. (2011). Strain–life curves of steels and methods for determining the curve parameters. part 2. methods based on the use of artificial neural networks. *Strength of Materials*, 43(1), 1.

Wong, W. A. (1984). *Monotonic and cyclic fatigue properties of automotive aluminum alloys*. Technical report, SAE Technical Paper.

RESPONSIBILITY NOTICE

The authors are the only responsible for the printed material included in this paper.